We are IntechOpen, the world's leading publisher of Open Access books Built by scientists, for scientists

4,800
Open access books available

122,000
International authors and editors

135M
Downloads

Our authors are among the

154
Countries delivered to

TOP 1%
most cited scientists

12.2%
Contributors from top 500 universities

CLARIVATE ANALYTICS BOOK CITATION INDEX INDEXED

WEB OF SCIENCE™

Selection of our books indexed in the Book Citation Index in Web of Science™ Core Collection (BKCI)

Interested in publishing with us?
Contact book.department@intechopen.com

Numbers displayed above are based on latest data collected.
For more information visit www.intechopen.com

Chapter

Vortices in Rotating and Gravitating Gas Disk and in a Protoplanetary Disk

Martin G. Abrahamyan

Abstract

Nonlinear equations describing dynamics of 2D vortices are very important in the physics of the ocean and the atmosphere and in plasma physics and Astrophysics. Here linear and nonlinear 2D vortex perturbations of gravitating and light gaseous disks are examined in the geostrophic and post-geostrophic approximations. In the frame of geostrophic approximation, it is shown that the vortex with positive velocity circulation is characterized by low pressure with negative excess mass density of substance. Vortex with negative circulation has higher pressure and is a relatively tight formation with the positive excess mass density. In the post-geostrophic approximation, structures of the isolated monopole and dipole vortex (modons) solutions of these equations are studied. Two types of mass distributions in dipole vortices are found. The first type of modon is characterized by an asymmetrically positioned single circular densification and one rarefaction. The second type is characterized by two asymmetrically positioned densifications and two rarefactions, where the second densification-rarefaction pair is crescent shaped. The constant density contours of a dipole vortex in a light gas disk coincide with the streamlines of the vortex; in a self-gravitating disk, the constant density contours in the vortex do not coincide with streamlines. Possible manifestations of monopole and dipole vortices in astrophysical objects are discussed. Vortices play decisive role in the process of planet formation. Gas in a protoplanetary disk practically moves on sub-Keplerian speeds. Rigid particles, under the action of a head wind drags, lose the angular momentum and energy. As a result, the ~10 cm to meter-sized particles drift to the central star for hundreds of years. Long-lived vortical structures in gas disk are a possible way to concentrate the ~10 cm to meter sized particles and to grow up them in planetesimal. Here the effect of anticyclonic Burgers vortex on formation of planetesimals in a protoplanetary dusty disc in local approach is also considered. It is shown that the Burgers vortex with homogeneously rotating kernel and a converging radial stream of substance can effectively accumulate in its nuclear area the meter-sized rigid particles of total mass $\sim 10^{28}$ g for characteristic time $\sim 10^{6}$ year.

Keywords: anticyclone, Burgers vortex, dipole, gravitating disk, monopole, planetesimals, protoplanetary disk, vortex

1. Introduction

Nonlinear equations describing dynamics of 2D vortices are important in the physics of the ocean and the atmosphere, in plasma physics, and in astrophysics. The same type of nonlinear equations describes these vortical structures. In fluid dynamics, Hasegawa-Mima equation is well-known [1].

$$\frac{\partial}{\partial t}(1-\Delta)\psi - v_0\frac{\partial \psi}{\partial y} - (\boldsymbol{e}_z \times \nabla\psi)\nabla\Delta\psi = 0, \tag{1}$$

which describes the nonlinear Rossby waves in the atmosphere [2] and drift nonlinear waves in plasma [3]. Here $\psi(x,y,z)$ is a stream function: $v = e_z \times \nabla\psi$. In plasma physics ψ is the electric potential, and constant v_0 is defined by equilibrium density gradient.

The exact solution of the equation, describing a stationary solitary dipole vortex (modon) drifting along the y-axis on rotating shallow water, was obtained in [4]. The same type of solutions later received a large number of similar equations [5–10].

Nonlinear vortex disturbances of uniformly rotating gravitating gaseous disk were considered in [9]. For short-scale (much smaller than the Jeans wavelength: $\lambda \ll \lambda_J$) and long-scale $\lambda \gg \lambda_J$ perturbations, nonlinear equation turns into Eq. (1).

IR, submillimeter, and centimeter radiation of protoplanetary disk analyses shows that vortices serve as incubators for the growth of dust particles and formation of planetesimals [15–18]. The initial stage of growth probably proceeds through the nucleation of submicron-sized dust grains from the primordial nebula, which then forms the monomers of fractal dust aggregates up to ~1 mm to ~10 cm for characteristic time of an order of 10^3 years [19, 20]. The best astrophysical evidence for grain growth to specified sizes is the detection of 3.5 cm dust emission from the face-on disk of radius 225 AU round classical T Tauri star TW Hya [21]. When the planetesimals reached a size of about 1 km, they began to attract other smaller bodies due to their gravity.

In models of protoplanetary disks, gas practically moves on sub-Keplerian speeds. Rigid particles, under the action of a head wind drag, lose the angular momentum and energy. As a result, the ~10 cm to meter-sized particles drift to the central star for hundreds of years, that is, much less than the lifetime of a disk which makes several millions of years [22, 23].

Long-lived vortical structures in gas disk are a possible way to concentrate the ~10 cm to meter-sized particles and to grow up them in planetesimal. Similar effect of vortices on the Earth was observed in special laboratories and also in the ocean [24].

In some areas of the stratified protoplanetary disks, the current has a 2D turbulent character. An attractive feature of such hydrodynamic current consists in the fact that in it, through a background of small whirlpools, long-living vortices will spontaneously be formed without requirement of special initial conditions [25–27]. In laboratory experiments [28, 29], formation of Burgers vortex, which will be considered here, is often observed in 2D turbulent flows. Anticyclonic vortices in a protoplanetary disk merge with each other and amplify, while cyclonic ones are destroyed by a shear flow [30].

In cylindrical system of coordinates (r, θ, z), the Burgers vortex is defined as

$$v_r = -Ar, v_\theta = \omega r_0{}^2\left[1 - \exp\left(-r^2/r_0^2\right)\right]/r, \quad v_z = 2Az. \tag{2}$$

This is a vortex with a converging stream of substance to its center with gradient –A, ω and r_0 as the circulation and the size of a trunk of a vortex. Rotation of a

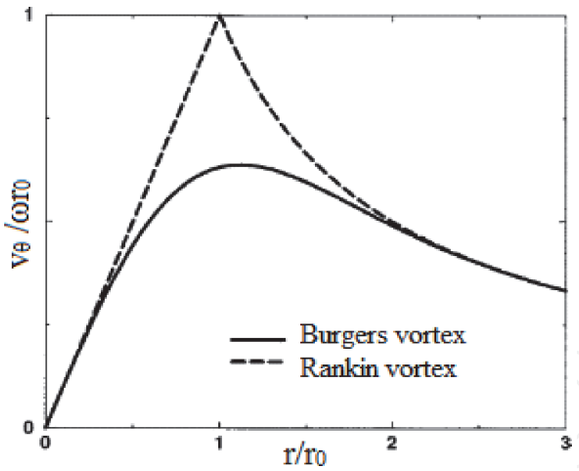

Figure 1.
Rotational velocity profiles of Burgers and Rankin vortices.

vortex trunk is almost uniform, then falls down under hyperbolic law, and at distance $r_{eff} = 4.5r_0$ (effective radius of vortex) makes 1/3 of the maximum value of v_θ (**Figure 1**). The asymptotic behavior of Burgers vortex in small and big distances from the vortex center represents the Rankin vortex [12, 13].

2. Magnitude of some parameters of circumstellar disks

A typical circumstellar disk is a few hundred AU (astronomical unit, 1 AU = 1.5 10^{13} cm) in size. It is mainly composed of hydrogen and helium gas. We consider a vortex in such axially symmetrical viscous accretion disk with effective temperature T and gas density ρ, of almost Keplerian rotation.

The sound speed in gas is estimated by

$$c_s = \sqrt{\gamma kT/m_H} \approx (\gamma T/100K)^{1/2} km/s, \tag{3}$$

where $\gamma = 1.4$ is the gas adiabatic index, k is Boltzmann constant, m_H is hydrogen atom mass.

In a vertical direction, the gas is in hydrostatic balance with a characteristic scale height:

$$H \sim \frac{c_s}{\Omega} \approx 0.03\left(\frac{T}{100K}\right)^{1/2}\left(\frac{M_\odot}{M}\right)^{1/2}\left(\frac{R}{AU}\right)^{3/2} AU. \tag{4}$$

The thickness-to-radius ratio (aspect ratio) is usually ~ 1/10 and increases slowly with radius, R. The superficial density of the gas in a disk can be estimated as $\Sigma \approx 2H\rho$.

In "α-model" of accretion disk [31], the expense of gas occurs with a speed $dm/dt = 3\pi\nu\Sigma$, where ν is the kinematic viscosity of gas, $\nu = \alpha c_s H$.

The dynamic time scale of a disk is

$$\tau \sim \frac{1}{\Omega} \approx \frac{1}{5}\left(\frac{M_\odot}{M}\right)^{1/2}\left(\frac{R}{AU}\right)^{3/2} yr \tag{5}$$

For Keplerian disk, radial momentum equation solution yields to a difference between the speeds of rigid particles and surrounding gas [32]. In a thin gas disk ($c_s \ll \Omega R$), rigid particles drift relative to gas with a speed

$$\frac{\Delta v}{c_s} \sim \frac{c_s}{\Omega R} \approx 0.03\left(\frac{T}{100K}\right)^{1/2}\left(\frac{M_\odot}{M}\right)^{1/2}\left(\frac{R}{AU}\right)^{1/2}. \quad (6)$$

At $c_s \sim 1$km/s, typical drift speed is of order 30 m/s. The characteristic scale of drift time [22, 23] almost by two orders surpasses the dynamic time: $\tau_d \sim r/\Delta v \sim$ (R/A.E.) 10^2yr.

For a characteristic time $\tau_s \sim \Sigma/\alpha\Omega\rho*$ [33], where ρ^* is the mass density of a particle, dust settled on a midplane of a disk. The characteristic time between collisions of rigid particles among themselves is estimated as $\tau_{col} \sim D\rho*/\Sigma*\Omega$, where D is the diameter of a particle and Σ^* is the superficial density of rigid particles in a disk which is more than by two orders less than a disk Σ.

Viscous dissipation and orbital shear limit the sizes of a vortex. Viscous dissipation destroys vortices of sizes less than the viscous scale [34]:

$$L_\nu = \frac{\alpha c_s H}{v_\theta} \approx 0.003\left(\frac{\alpha}{0.01}\right)\left(\frac{0.1c_s}{v_\theta}\right)\left(\frac{M_\odot}{M}\right)^{1/2}\left(\frac{R}{AU}\right)^{3/2} AU, \quad (7)$$

where v_θ is the rotational speed of a vortex.

The Keplerian shear flow forbids the formation of circular structures with the sizes larger than the shear length scale:

$$L_{shear} = \sqrt{v_\theta\left|\frac{d\Omega}{dR}\right|^{-1}} \approx 0.05\left(\frac{v_\theta}{0.1c_s}\right)^{1/2}\left(\frac{M_\odot}{M}\right)^{1/4}\left(\frac{R}{AU}\right)^{5/4} AU. \quad (8)$$

The vortices, whose sizes surpass L_{shear}, are extended in an azimuthal direction that allows them to survive longer. In [35] we have shown the possibility of formation in a disk extended in an azimuthal direction three-axis ellipsoidal vortex, with a linear field of circulation, similar to Riemann S ellipsoids [36]. However, in a disk round the central star of solar mass, at distance 30 AU, the vortex of characteristic speed of rotation, $0.01c_s$, can be circular and have the size of an order of ~1 AU.

In a gas disk, drag force on rigid particles from gas is exposed, which, depending on size of a particle, is expressed either by Stokes or Epstein's formula (see, e.g., [29]).

Here our main results obtained by investigations of the linear and nonlinear perturbation equations of differentially rotating gravitating gaseous disk in geostrophic and post-geostrophic approximations are presented [11], as well as the results on formation of planetesimals by Burgers vortex in a protoplanetary disk [30].

3. Model and basic equations for linear perturbations

Consider at first a gravitating pure gas disk of mass density $\rho(r)$, which rotates with angular velocity $\Omega(r)$ around the z-axis. Explore 2D perturbations in plane of the disk, ignoring its vertical structure. Present any characteristic functions of the disk as $f_0(r) + f(r, \varphi, t)$, where $f_0(r)$ describes the equilibrium state and $f(r, \varphi, t)$ is a small but finite perturbation.

We will consider isentropic perturbations (S = constant) and therefore enthalpy H(S, P) = H(P),

where P is the pressure and

$$dH = dP/\rho = c_s{}^2 d\rho/\rho, \quad (9)$$

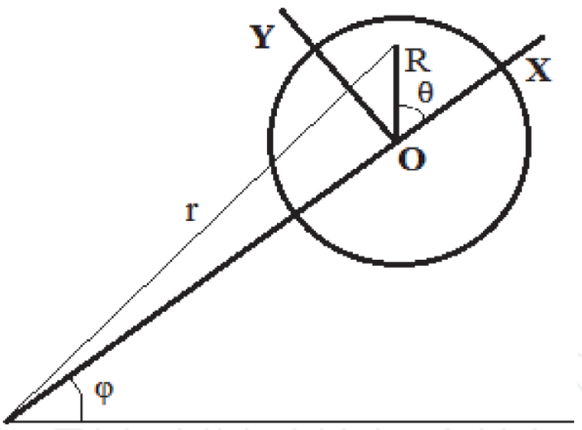

Figure 2.
The local frame of reference 1.

where c_s is the sound speed. Evidently, Eq. (9) is the equation of state of disk substance.

Perturbations of the disk in a rotating with angular velocity $\Omega_0 \equiv \Omega(r_0)$ cylindrical coordinate system (**Figure 2**) are described by 2D hydrodynamic equations[1]:

$$d\mathbf{v}/dt + 2\Omega_0 \mathbf{e}_z \times \mathbf{v} + \mathbf{e}_\varphi v_r r\Omega' + \nabla\Phi = 0, \tag{10}$$

$$d\rho/dt + \rho\nabla(\mathbf{v}) = 0, \tag{11}$$

where the velocity was presented in the form of

$$\mathbf{V}_0 \equiv \mathbf{e}_\varphi(\Omega - \Omega_0)r,$$

Φ is the sum of perturbations of gravitational potential U and enthalpy

$$\Phi \equiv U + H, \tag{12}$$

$$d/dt = \partial/\partial t + V_0\partial/r\partial\varphi + \mathbf{v}\nabla; \tag{13}$$

and the Poisson equation is

$$\Delta U = 4\pi G\rho, \tag{14}$$

In Eq. (10) we have used the radial equilibrium condition for the disk:

$$\Omega^2 r = d\Phi_0/dr. \tag{15}$$

Taking into account Eq. (9), the continuity Eq. (11) can be written as

$$dH/dt + c_s{}^2\nabla\mathbf{v} = 0. \tag{16}$$

Taking operator **curl** on Eq. (10) and then by combining the equation of continuity, after simple transformation, we obtain

$$d/dt\{[curl_z\mathbf{v} + 2\Omega + r\Omega']/\rho\} = 0. \tag{17}$$

[1] Here and below the bar indicates the differentiation of equilibrium parameters of the disk on the radial coordinate r.

The expression in the curly brackets in this equation is a generalized vortencity. The equation shows that for 2D isentropic perturbations, generalized vortencity is conserved along the current lines. So for stationary perturbations, generalized vortencity is an arbitrary function of ψ:

$$(\mathrm{curl}_z\mathbf{v} + 2\Omega + r\Omega')/\rho = B(\psi). \tag{18}$$

In a uniformly rotating ($\Omega = \text{const.}$) gravitating disk, no drifting stationary vortex solution can be obtained without specifying the function $B(\psi)$, because Eq. (18) can be represented as a Jacobean $J\{\psi, (\mathrm{curl}_z\mathbf{v} + 2\Omega)/\rho\} = 0$, which satisfies the arbitrary circularly symmetric vortex disturbance around point O.

4. Vortices in the geostrophic approximation

This approach assumes that Coriolis forces and gravity balance the pressure gradient in the disk.

Then from the equation of motion (17), we get the perturbed geostrophic velocity:

$$\mathbf{v}_G = (1/2\Omega_0)\mathbf{e}_z \times \nabla\Phi. \tag{19}$$

Using the last, Eq. (18) takes the form

$$(1/2\Omega_0\rho)\ \Delta\Phi + (2\Omega + r\Omega_0{}')/\rho = B(\psi). \tag{20}$$

In further analysis of this topic, we will introduce the local Cartesian coordinate system (X,Y) such that (**Figure 2**)

$$\partial/\partial x = \partial/\partial r, \partial/\partial y = \partial/r\partial\varphi, \tag{21}$$

and will explore the vortical perturbations around a point O in a linear approximation.

The stream function $\psi(x, y)$ of perturbed velocity (19) is expressed through perturbations Φ by the following formula:

$$\psi = \Phi/2\Omega_0. \tag{22}$$

Imagine around a point O function $\rho(x)$ and $\Omega(x)$ in the form of

$$\rho(x) = \rho_0(r_0) + x\rho_0' + \rho(x, y); \Omega(x) = \Omega_0 + x\Omega_0'. \tag{23}$$

In this case $V_0 \approx r_0\Omega_0' x$.

Perturbations of density and enthalpy (9) in linear approach are connected by the following formula:

$$\rho(x, y) = \rho_0 H(x, y)/{c_s}^2, \tag{24}$$

Then Eq. (13) with an accuracy to a constant term will be in the form of

$$B(\psi) = {\rho_0}^{-1}\{\Delta\psi\text{-}{\kappa_0}^2{k_R}^2 H/2\Omega_0\Omega^2) + x\beta\}, \tag{25}$$

where $k_R = \Omega_0/c_s$ is the Rossby wave number, $\kappa_0{}^2 = 2\Omega_0\left(2\Omega_0 + r_0\Omega_0'\right)$ is the square of the epicyclical frequency, and

$$\beta \equiv 3\Omega_0' - \kappa_0{}^2\rho_0'/2\Omega_0\rho_0. \tag{26}$$

If to take the relationship of density perturbations with perturbations of gravitational potential using Poisson equation

$$\rho(x, y) = \Delta U(x, y)/4\pi(G),$$

instead of Eq. (25), we obtain the equation

$$B(\psi) = \rho_0{}^{-1}\left\{\Delta\psi - \kappa_0{}^2\Delta U/2\Omega_0\ \omega_J{}^2 + x\beta\right\}, \tag{27}$$

where $\omega_J{}^2 \equiv 4\pi G\rho_0$ is the square of the Jeans frequency.

The order of magnitude of $|H/U|$ can be estimated using the definition $c_s{}^2 = (dP_0/d\rho_0)$ and $|\Delta\Phi| = k^2\Phi$.

where k is wavenumber of perturbations

$$|H/U| \approx k^2 c_s{}^2/\omega_J{}^2 = k^2/k_J{}^2, \tag{28}$$

where $k_J = \omega_J/c_s$ is the Jeans wavenumber. Eq. (28) shows that the case $|H| \gg |U|$ describes the small-scale disturbances: matching $k^2/k_J{}^2 \gg 1$, or $\lambda \ll \lambda_J$. In this case $\psi = H/2\Omega_0 \equiv h$, and Eq. (25) takes the form

$$B(h) = \rho_0^{-1}\left\{\Delta h - \left(\kappa_0^2 k_R^2/\Omega_0^2\right)h + xb\right\}. \tag{29}$$

Limit $|H| \ll |U|$corresponds to the large-scale perturbations $-\lambda \gg \lambda_J$. Then $\psi = U/2\Omega_0 \equiv \phi$, and Eq. (27) turns into

$$B(\phi) = \rho_0^{-1}\left\{\left(1 - \kappa_0^2/\omega_J^2\right)\Delta\varphi + xb\right\}. \tag{30}$$

By selection of function B, we can explore the stationary vortex solutions of Eqs. (29) and (30).

Let's take a look at the simplest case of uniformly rotating disk of homogeneous density, $\beta = 0$, $\kappa_0^2 = 4\Omega_0^2$, when the vortencity is constant and is equal to $\Gamma/\rho_0\pi a^2$ where Γ is the velocity circulation. We assume that the velocity circulation Γ differs from zero only in a circle of radius $a(\ll r_0)$ around point O. Using now the polar coordinates $(R, \theta) : x = R\cos\theta, y = R\sin\theta$ (**Figure 2**), the equation for disturbances (29) can be written as

$$\Delta h - 4k_R^2 = \begin{cases} \Gamma/\pi\alpha^2, & R \le a \\ 0, & R \ge a \end{cases} \tag{31}$$

which gives a circularly symmetric solution for relative perturbed density of mass

$$\frac{\rho}{\rho_0} = -\frac{\Gamma}{\pi a s c_s}\begin{cases} 1 - \dfrac{K_1(s)I_0(sR/a)}{K_1(s)I_0(s) + I_1(s)K_0(s)}, & R \le a \\ \dfrac{I_1(s)K_0(sR/a)}{K_1(s)I_0(s) + I_1(s)K_0(s)}, & R \ge a \end{cases} \tag{32}$$

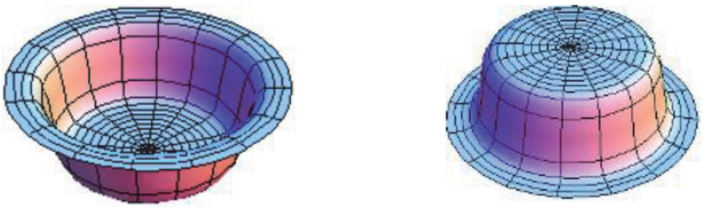

$\Gamma > 0.$ $\Gamma < 0.$

Figure 3.
3D image of relative density perturbations of whirlwind in the range $0 \le R/a < 1.4$ *for* $2a\mathrm{k_R} = 20$.

where $\mathrm{s} \equiv 2a\,\mathrm{k_R}$. This is a monopole vortex with the following perturbed velocity field:

$$v_\theta = \frac{\Gamma}{\pi a s}\begin{cases} \dfrac{K_1(s)I_1(sR/a)}{K_1(s)I_0(s)+I_1(s)K_0(s)}, & R \le a \\ \dfrac{I_1(s)K_1(sR/a)}{K_1(s)I_0(s)+I_1(s)K_0(s)}, & R \ge a. \end{cases} \tag{33}$$

Note that the vortices with positive and negative velocity circulation Γ have different properties. Whirlwind with positive circulation is characterized by low pressure, with negative excess mass density of substance. Vortex with negative circulation has a higher pressure and relatively tight formation with the positive excess mass density.

To illustrate these results, we will take into account the fact that the Rossby wavenumber usually is of the order of the inverse thickness of the disk. Considering that the size of the vortex a as the disk thickness order, we will get for the Bessel function argument $2a\mathrm{k_R} \approx 12$. **Figure 2** shows 3D image relative density perturbations in monopole whirlwind occupying the region $0 \le R/a \le 1.35$, for the value of the argument $\mathrm{s} = 12$. This vortex is a retrograde-circulating rarefaction around the center O condensation in the case of $\Gamma < 0$ and prograde-circulating rarefaction in the case of $\Gamma > 0$ (**Figure 3**). The decrease of density in the area $R > a$ of larger vortex is steeper. If the size of the vortex tends to zero, we get a simple classic case of point vortex.

For long-scale perturbations (33), the Rankin vortex velocity profile is given [12, 13]:

$$v = \frac{\Gamma}{2\pi\gamma\alpha}\begin{cases} R/a, & R \le a \\ a/R, & R \ge a. \end{cases} \tag{34}$$

where $\gamma = 1 - \Omega^2/\pi\mathrm{G}\rho_0$.

5. Vortices in the post-geostrophic approximation

In this section, we will get nonlinear perturbation equation, taking into account the inertia term in the equation of motion (10) for homogeneously rotating disk. The cross product of Eq. (10) with $\mathrm{e_z}$: $\mathrm{e_z} \times$ Eq. (10), gives

$$\mathbf{v} = \mathbf{v}_\mathrm{G} + \mathbf{v}_\mathrm{I}, \tag{35}$$

where the first term is geostrophic speed (19) and the second is

$$\mathbf{v}_I \equiv (1/2\Omega_0)\mathbf{e}_z \times d\mathbf{v}/dt. \tag{36}$$

Substituting Eq. (35) to Eq. (36) and taking approximation $d/dt \ll \Omega$ (slowly varying perturbations), dropping the term $\mathbf{v}_I\nabla$ in the expression (13) for d/dt, we get.

$$\mathbf{v}_I = \left(1/4\Omega_0{}^2\right)\mathbf{e_z} \times d[\mathbf{e}_z \times \nabla\Phi]dt. \tag{37}$$

With the use of Eqs. (19) and (34), we find

$$\nabla\mathbf{v}_G = 0, \tag{38}$$

$$\nabla\mathbf{v}_I = -\left(1/4\Omega_0{}^2\right)L\Delta\Phi. \tag{39}$$

where

$$L \equiv \partial/\partial t + (1/2\Omega_0)(\nabla\Phi \times \nabla)_z. \tag{40}$$

The continuity equation now takes the form

$$d\left(\rho_+\rho_0\right)/dt + \left(\rho_+\rho_0\right)\nabla\mathbf{v}_I = 0, \tag{41}$$

or, using Eqs. (14), (20), and (21)

$$L\rho - \left(\rho_0/4\Omega_0{}^2\right)L\Delta\Phi. \tag{42}$$

Here we have served the terms that are of second order in perturbed amplitude and neglected terms of highest order.

Using the Poisson equation, we get from Eq. (42) the basic nonlinear equation

$$L\Delta U - ½\alpha\, L\Delta\Phi + \beta\partial\Phi/r\partial\varphi = 0, \tag{43}$$

where

$$\alpha \equiv \omega_J{}^2/2\Omega_0{}^2; \alpha' \equiv d\alpha/dr; \beta = \alpha'\Omega_0; \omega_J{}^2 \equiv 4\pi G\rho_0 \tag{44}$$

In view of the assessment (28), for short-scale perturbations ($\lambda \ll \lambda_J$), Eq. (42) takes the form

$$\left(\frac{\partial}{\partial t} + \frac{2}{2\Omega_0}(\nabla H \times \nabla)_z\right)\Delta H + \frac{2\beta}{\alpha}\frac{1}{r}\frac{\partial H}{\partial\varphi} = 0. \tag{45}$$

On the limit $|H| \ll |U|$ that corresponds to large-scale disturbances: $\lambda \gg \lambda_J$, Eq. (42) turns into [9].

$$\left(\frac{\partial}{\partial t} + \frac{2}{2\Omega_0}(\nabla U \times \nabla)_z\right)\Delta U + \frac{2\beta}{\alpha - 2}\frac{1}{r}\frac{\partial H}{\partial\varphi} = 0. \tag{46}$$

Eqs. (45) and (46) have the same structure differing only by their coefficients, and are Hasegawa-Mima type (see Eq. (1)).

6. A solitary dipole vortex

In a Cartesian coordinate system (X,Y) (**Figure 2**), we will look for stationary solutions of Eq. (45) (and (46)) in a small neighborhood of the guiding center O

with a radius of $a \ll r_0$ in the form of a vortex drifting in y-direction at a constant speed u. Introducing the wave variable

$$\eta = \text{y-ut} \tag{47}$$

Eq. (46) can be rewritten in the form

$$\left\{\partial/\partial\eta - A(\nabla U \times \nabla)_z\right\}\delta U = \Lambda\partial U/\partial\eta, \tag{48}$$

or in the form of the Jacobean

$$J(\text{U-x}/A, \Delta U + \Lambda x/A) = 0, \tag{49}$$

where

$$(A)^{-1} = 2u\Omega, \Lambda = -4{\Omega_0}^2 A(\ln|\alpha - 2|)'. \tag{50}$$

On basis of Eq. (49)

$$\Delta U + \Lambda x/A = F(U - x/A), \tag{51}$$

where F is an arbitrary function. As we are interested in the restricted solutions, then in the limit of large values η, solution U should vanish for arbitrary values x; therefore

$$F(-x/A) = -\Lambda x/(A). \tag{52}$$

We will assume that the function F (51) in the equation is linear not only for large η but across the whole plane (x, η). In general, F can be represented as $\propto (U - x/A)$. Introducing polar coordinates $R, \theta : x = R\cos\theta, \eta = R\sin\theta$, we can write Eq. (49) in the form

$$\left(\Delta + k^2\right)U = A^{-1}\left(k^2 - \Lambda\right)R\cos\ \theta, \quad R\ \leq a, \tag{53}$$

$$\left(\Delta - p^2\right)U = 0, \quad R\ \geq a, \tag{54}$$

where k and p are real constants. Soon the sense of splitting the (R, θ) plane into two parts will be obvious. Eq. (54) turns out to be uniform, because for a restricted solution, we have $U \to 0$ for large R. This condition implies

$$p^2 = -\Lambda. \tag{55}$$

Eqs. (53) and (54) have the following stationary solution [9]:

$$U(R,\theta) = \Omega ua\begin{cases}\left[\left(1 - \dfrac{s^2}{g^2}\right)\dfrac{R}{a} + \dfrac{s^2}{g^2}\dfrac{J_1(gR/a)}{J_1(g)}\right]\cos\theta, & R \leq a \\ -\dfrac{K_1(sR/a)}{K_1(s)}\cos\theta & R \geq a\end{cases} \tag{56}$$

where J_1 and K_1 are Bessel and Macdonald functions, respectively, and $g = ka$ and $s = pa$ are connected by "dispersion equation" which is transcendental

$$(J)_1(g)(K)_3(s) + (J)_3(g)(K)_1(s) = 0. \tag{57}$$

For long-scale perturbations

$$s^2 = \left(2\Omega(a)^2/u\right)(\ln|\alpha - 2|)', \tag{58}$$

while for small-scale disturbances

$$U \to H = c_s{}^2\rho|\rho_0, \text{and } s^2 = \left(2\Omega^2 a/u\right)(\ln\alpha)'. \tag{59}$$

From Eqs. (56) and (19), we get the velocity field of a vortex in the form

$$v_R = -\frac{1}{2\Omega}\frac{\partial\Phi}{R\partial\theta} = u\begin{cases}\left[1-\frac{s^2}{g^2}\left(1-\frac{aJ_1(gR/a)}{RJ_1(g)}\right)\right]\sin\theta, & R\le a\\ \frac{aK_1'(sR/a)}{RK_1(s)}\sin\theta, & R\ge a\end{cases} \tag{60}$$

$$v_\theta = \frac{1}{2\Omega}\frac{\partial\Phi}{\partial R} = u\begin{cases}\left[1-\frac{s^2}{g^2}\left(1-g\frac{J_1'(gR/a)}{J_1(g)}\right)\right]\cos\theta, & R\le a\\ \frac{sK_1{}'(sR/a)}{K_1(s)}\cos\theta, & R\ge a\end{cases} \tag{61}$$

Moreover, the condition (57) is derived from the requirements of continuity (61) on the circle $R = a$.

The current lines are determined by $dR/v_r = Rd\theta/v_\theta$ that gives

$$const. = \begin{cases}\left[\left(1-\frac{s^2}{g^2}\right)\frac{R}{a}+\frac{s^2}{g^2}\frac{J_1(gR/a)}{J_1(g)}\right]\sin 2\theta, & R\le a\\ \frac{K_1(sR/a)}{K_1(s)}\sin 2\theta, & R\ge a.\end{cases} \tag{62}$$

Figure 4 shows the current lines of drifting solitary dipole vortex, the appropriate formula (62).

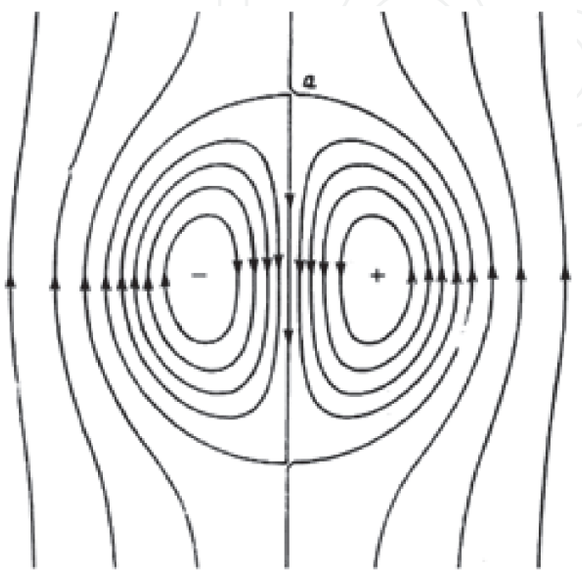

Figure 4.
The stream lines of solitary dipole vortex [9].

7. The contours of constant density

As shown in Section 3, $\Phi/2\Omega$ is the current function of perturbed speed, ψ in the case of short-scale disturbances $\Phi = H$. Then we have the $\psi = H(\rho)/2\Omega$; the constant values of the contours of constant density ρ match the lines of the current $\psi =$ constant: in short-scale modon, substance flows along the lines of constant density.

In the long-scale limit, $\Phi = U$ and $\psi = U/2\Omega$. Therefore, in this case the current lines coincide with equipotentials of the gravitational field, not with the contours of constant density. The last can be found using the Poisson equation:

$$\Delta\psi = 2\pi G\rho/\Omega. \tag{63}$$

Since equipotentials U = constant, generally speaking, do not coincide with the contours of constant density, it follows that the stream lines ψ = constant do not coincide with the contours of constant density.

Define the contours of constant density of modon. Relative density perturbations in the short-scale range are expressed by the following formula:

$$\sigma = \rho/\rho_0 = \beta_{sw} H/au\Omega, \text{where}\, \beta_{sw} \equiv au\Omega/{c_s}^2. \tag{64}$$

The relative perturbed density in long-scale range turns out to be in the form

$$\sigma = \frac{1}{\omega_J^2}\Delta\psi = \beta_{lw}\begin{cases}\dfrac{J_1(gR/a)}{J_1(g)}\cos\theta, & R \le a\\[2ex] \dfrac{K_1(sR/a)}{K_1(s)}\cos\theta, & R \ge a\end{cases} \tag{65}$$

where

$$\beta_{lw} \equiv -u\Omega s^2/a{\omega_J}^2 = -(\ln|\alpha - 2|)''/\alpha. \tag{66}$$

To illustrate, consider a logarithmic model of the disk, describing in equilibrium by the following functions of potential, mass density, and angular velocity:

$$\begin{aligned} U_0(r) = \tfrac{1}{2}{v_0}^2 \ln\left({R_c}^2 + r^2\right), \rho_0(r) = {v_0}^2 R^2/2\pi G\left({R_c}^2 + r^2\right),\\ \Omega^2 = {v_0}^2/\left({R_c}^2 + r^2\right), \end{aligned} \tag{67}$$

where R_c and v_0 are constants, rotation of a disk in the small area $(a \ll R_c)$ can be considered as uniform, and β_{lw} for this model turns out to be equal to

$$\beta_{lw} \approx 8ar/3{R_{(c)}}^2 \approx 8a(R_c + R\cos\theta)/3{R_c}^2, \tag{68}$$

where we used the relation ${r}^2 \approx {R_c}^2 + 2RR_c\cos\theta$, by placing the center O in $R = R_c$.

For illustrations of a perturbed density distribution in dipole vortex (65), we used the following solutions of "dispersion equation" (57): (g,s) = (4.0, 1.52); (4.2, 2.90); (4.5, 6.0); (4.7, 10.0).

The curves in **Figure 5** show perturbed density as a function of dimensionless distance R/a from the guiding center O in the short-scale (curves increasing towards the center) and in the long-scale (curves descending towards the center) limit.

The density distribution is antisymmetrical to the guiding center. Depending on the choice of the dispersion curve (57) range, there are two types of mass distribution in dipole vortex. One is antisymmetrically located almost round condensation,

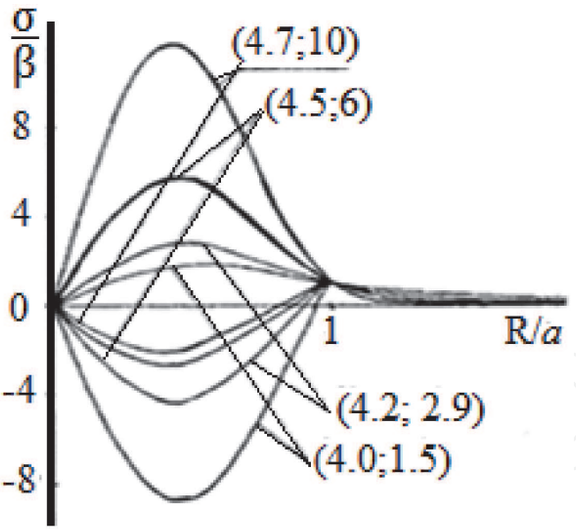

Figure 5.
Dependence of relative perturbed density from the dimensionless distance R/a in short-scale and long-scale modons.

and one rarefaction (**Figure 6**) characterizes the first type. The second type is characterized by the two antisymmetrically located condensations and two rarefactions, and second condensation-rarefaction pair has sickle-form (**Figure 7**). For small values g and s, the short-scale modon is of the second type, with distinctive two condensations (see **Figure 8**). In the middle part of the dispersion curve, the short-scale and long-scale modons have roughly the same structure. They have one antisymmetrical located prominent pair of condensation-rarefaction and another weak pair of sickle forms. For large values of g and s, the short-scale modon is the first type and has the character of a cyclone-anticyclone couple; the long-scale one is the second type and is characterized by a nearly round and sickle-shaped condensations. In laboratory experiments, the solitary dipole vortices on shallow water,

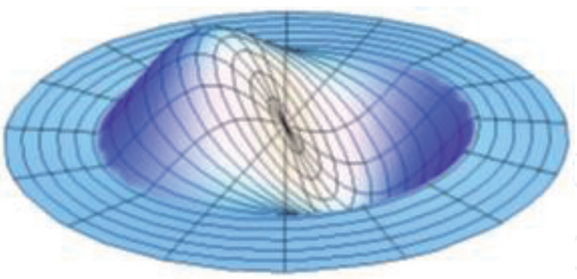

Figure 6.
3D image of density distribution in the first type modon.

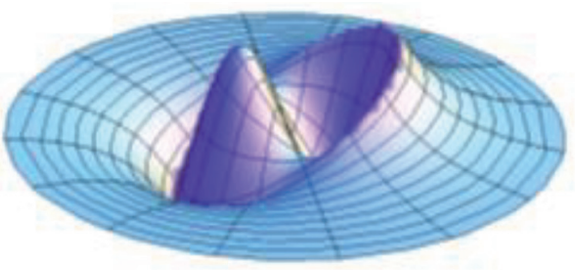

Figure 7.
3D image of density distribution in the second type modon.

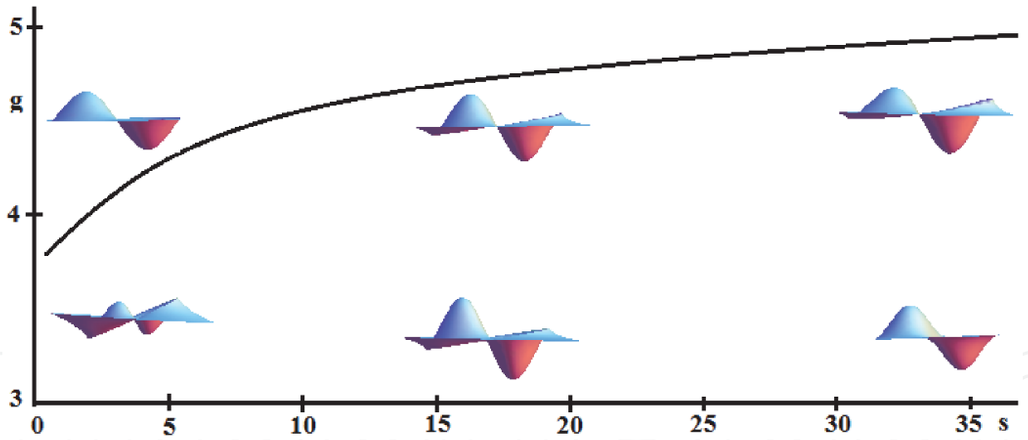

Figure 8.
"Dispersive curve"—the solution of Eq. (57). In the three ranges of the curve, 3D images described the relative perturbed density of modon in short-scale (lower row) and long-scale (upper row) limits. The blue color indicates condensations, and red color indicates rarefactions.

obviously, are the short-scale modons of the first type with the asymmetry between high- and low-pressure centers.

Let's estimate the masses of condensations in long-scale modon:

$$m_1 = \frac{2\pi h p_0}{J_1(g)}\beta_{lw}\int_{\pi/2}^{3\pi/2}\cos\theta d\theta\int_0^{x_1}J_1(gx)xdx = \frac{4\pi a^2 h p_0}{J_1(g)}\beta_{lw}J_0(gx_1)H_1(gx_1), \qquad (69)$$

where $x = R/(a)$, h is the thickness of the gas disk, $H_1(gx)$ is the Struve function of the first order, and x_1 is the root of equation $J_1(gx_1) = 0$. Similarly

$$m_2 = \frac{2\pi a^2 h\rho_0}{J_1(g)}\beta_{lw}\int_{-\pi/2}^{\pi/2}\cos\theta d\theta\int_{x_1}^{1}J_1(gx)xdx + \frac{2\pi a^2 h\rho_0}{K_1(s)}\beta_{lw}\int_{-\pi/2}^{\pi/2}\cos\theta d\theta\int_1^{\infty}K_1(sx)xdx. \qquad (70)$$

Numerical estimations show that the ratio of the masses of condensations in the long-scale modon, depending on values of parameters g and s, varies in the range $m_1/m_2 \sim 2-30$.

Now we will focus our attention on a role of vortices for the formation of planetesimals in a protoplanetary light dusty disk.

8. The Burgers vortex in local frame of reference

Let's use the local approach, choosing frame of reference, rotating with a disk with angular speed Ω_0 at distance R_0 round the central star of mass M. In this approach, assuming the effective radius of a vortex is much smaller than R_0, we will choose the Cartesian system of coordinates with center O (**Figure 9**), directing the y-axis to a star and the x-axis in direction of Keplerian flow of gas. We will present the disk rotation as

$$\Omega(R) \propto R^{-q}. \qquad (71)$$

In case when only the gravitation of the central star operates, rotation will be Keplerian with q = 3/2, and for homogeneously rotating disk, $q = 2$, i.e. $2 \geq q \geq 3/2$.

The substance stream in chosen frame of reference, has X component of speed $-iq\Omega_0 y$, centrifugal force is compensated by gravitation of the central star at distance

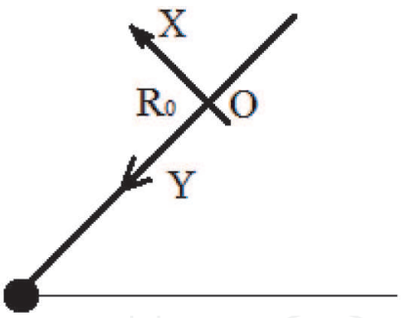

Figure 9.
The local frame of reference 2.

R_0, in other points their sum gives the tidal force $\mathbf{j}3\Omega_0{}^2y$. The vertical component of gravitation $-\Omega_0{}^2z$ is returning force along the z-axis.

In the local approach, the equation stationary isentropic shear flow of dusk viscous substance is described by Navier–Stokes and continuity equations:

$$(\mathbf{v}\nabla)\mathbf{v} = \mathbf{j}3\Omega_0{}^2y - \mathbf{k}\Omega_0{}^2z - 2\Omega_0 \times \mathbf{v} - \nabla h + \nu\Delta\mathbf{v} \tag{72}$$

$$\nabla(\rho\mathbf{v}) = 0, \tag{73}$$

where h is specific enthalpy $\left(h = \int \rho^{-1}dp\right)$ and **i**, **j**, and **k** are Cartesian unit vectors. The first term in the right-hand side of Eq. (72) is tidal acceleration, the second term is vertical gravitation, the third is acceleration of Coriolis, and the last is a viscous stress.

In the Cartesian coordinate system, the Burgers vortex (2) will be presented in the form

$$\begin{aligned} v_x &= -Ax - \omega r_0{}^2y\left[1 - \exp\left(-r^2/r_0{}^2\right)\right]/r^2, \\ v_y &= -Ay + \omega r_0{}^2x\left[1 - \exp\left(-r^2/r^2\right)\right]/r^2, \\ v_z &= 2Az, \end{aligned} \tag{74}$$

where $r^2 \equiv x^2 + y^2$.

9. Motion of rigid particles in Burgers vortex

Let us study the two-dimensional dynamics of dust rigid particles in a Burgers vortex. We will neglect the influence of rigid particles on dynamics of gas and the interaction of rigid particles among themselves.

As we consider centimeter- to meter-sized particles, then D considerably surpass the mean free path of gas molecules; therefore, the friction of rigid particles with gas will be described by Stokes drag force:

$$f = \beta(\mathbf{v} - \mathbf{u}), \text{where } \beta \equiv 18\ \rho\nu/\rho * D^2, \tag{75}$$

u = (dX/dt, dY/dt) is velocity of a particle, and X and Y are particle coordinates.

In a dimensionless form, the equation of motion of particles in the accepted approach looks like

$$du_x/dt = 2u_y + \gamma\left(v_x|_{r=(X,Y)} - u_x\right) - \partial h/\partial x\big|_{r=(X,Y)}, \tag{76}$$

$$du_y/dt = 3y - 2u_x + \gamma\left(v_y|_{r=(X,Y)} - u_y\right) - \partial h/\partial y\big|_{r=(X,Y),} \tag{77}$$

where γ is a dimensionless parameter

$$\gamma = \beta/\Omega_0 = 18\rho\nu/\rho * D^2\Omega_0. \tag{78}$$

In Eqs. (76) and (77) a characteristic length is accepted: the size of a trunk of a vortex r_0, for characteristic time and speed $-1/\Omega_0$ and $\Omega_0 r_0$, respectively.

In the vortex trunk area ($r^2/{r_0}^2 < 1$), the profile of rotation has uniform character:

$$v_x = -Ax - \omega y + O\left(r^2/{r_0}^2\right), v_y = -Ay + \omega x + O\left(r^2/{r_0}^2\right). \tag{79}$$

where A and ω are measured in unit Ω_0. Therefore

$$\partial h/\partial x = -\left(A^2 - \omega^2 - 2\omega\right)x - 2\,A(\omega + 1)y, \tag{80}$$

$$\partial h/\partial y = 2A(\omega + 1)x - \left(3 + A^2 - \omega^2 - 2\omega\right)y. \tag{81}$$

With the use of Eqs. (76)–(81), we receive the equations of motion of rigid particles in the field of a vortex trunk:

$$\begin{Bmatrix} \dot{X} \\ \dot{Y} \\ \dot{u}_x \\ \dot{u}_y \end{Bmatrix} = \begin{Bmatrix} 0 & 0 & 1 & 0 \\ 0 & 0 & 0 & 1 \\ a & b & -\gamma & 2 \\ -b & a & -2 & -\gamma \end{Bmatrix} \begin{Bmatrix} X \\ Y \\ u_x \\ u_y \end{Bmatrix}, \tag{82}$$

where

$$a = A(A - \gamma) - (\omega + 1)2 + 1; b = 2A(\omega + 1) - \gamma\omega. \tag{83}$$

From Eq. (82) it follows that the equilibrium position of rigid particles in a vortex trunk is its center $X = Y = 0$, where $u_x = u_y = 0$ and $\dot{u}_x = \dot{u}_y = 0$. Particles gradually come nearer to the center of the vortex by helicoidal trajectories.

For establishing the stability of this position of balance, it is necessary to require real parts of eigenvalues of a matrix in Eq. (82) to be zero or negative.

Eigenvalues are complex:

$$\Lambda_{1,2,3,4} = -\gamma/2 \mp i \pm \sqrt{\left[a - 1 + \gamma^2/4 \pm i(b - \gamma)\right]}, .$$

which gives stability condition

$$(b - \gamma)^2 + \gamma^2(a - 1) \le 0, \tag{84}$$

Taking into account Eq. (83), Eq. (84) leads to stability criterion $\gamma > A$, which for viscosity, ν, in a dimensional form, gives

$$\nu > \rho * AD^2/18\rho \tag{85}$$

Hence, the unique position of balance for rigid particles in a Burgers vortex is its center where all particles captured by a vortex will gather during the characteristic time:

$$\tau \sim \omega r_{eff}/A\sqrt{\beta\nu}. \tag{86}$$

The mass of the rigid particles captured by a vortex during this time is in the order

$$M_p \approx \pi {r_{eff}}^2 \Sigma *, \tag{87}$$

which forms a planetesimal.

10. The thickness of disk in nuclear area of Burgers vortex

So far we have considered the behavior of a whirlwind in a disk plane. However the whirlwind of Burgers is in 3D formation. We will discuss now a question on a thickness of a disk in the area where the Burgers vortex is located. For this purpose we will address a z-projection of the Navier–Stokes Eq. (72). Integrating this equation taking into account the formula for speed v_z, we will receive dependence enthalpy from the z coordinate:

$$h(z) = {c_{s0}}^2 - \left(4A^2 + {\Omega_0}^2\right)z^2/2,$$

where c_{s0} is a sound speed at the vortex center (enthalpy, $h_0 = {c_{s0}}^2$, at the center of vortex is estimated by Clapeyron equation) and Ω_0 is an angular speed of rotation of local frame of reference. Whence we obtain half thickness of a disk at the kernel area of a whirlwind:

$$z_0 = c_{s0}\left(2A^2 + {\Omega_0}^2/2\right)^{-1/2}. \tag{88}$$

The question arises whether the disk thickness in area of vortex localization changed. On radius of R_0 the half-thickness of Keplerian disk from (4) is of order $z_K \cong c_{s0}/2\Omega_0$. Therefore the relative thickening

$$\frac{\Delta z}{Z_K} \equiv \frac{Z_0}{Z_K} - 1 = \frac{2\sqrt{2}}{\sqrt{\left(1 + 4A^2/\Omega_0^2\right)}} - 1, \tag{89}$$

is positive if $A < 1.3\Omega_0$. This condition is carried out in all areas of a typical protoplanetary disk. Therefore, the disk in the area of localization of a whirlwind of Burgers is thicker.

11. Discussion and conclusion

First let's pay attention to the nontrivial structure of monopoly and dipole vortices in a rotating and gravitating pure gas disk. Monopole vortices (33) with mass distribution (32) are localized formations and can have positive and negative velocity circulation, and $\Gamma.\Gamma > 0$vortex, characterized by low pressure, has negative excess mass density of substance, in contrast of $\Gamma < 0$ vortex of higher pressure, with the positive excess mass density (see **Figure 3**).

More interesting are properties of solitary dipole vortex - modon (60), (61) with mass distribution (65) in short-scale and long-scale limits. There exist two types of mass distribution in dipole vortex. Anti-symmetrically located one almost round condensation and one rarefaction (**Figure 6**) characterizes the first type. The second type is characterized by the anti-symmetrical located two condensations and two rarefactions, and second condensation-rarefaction pair has sickle-form

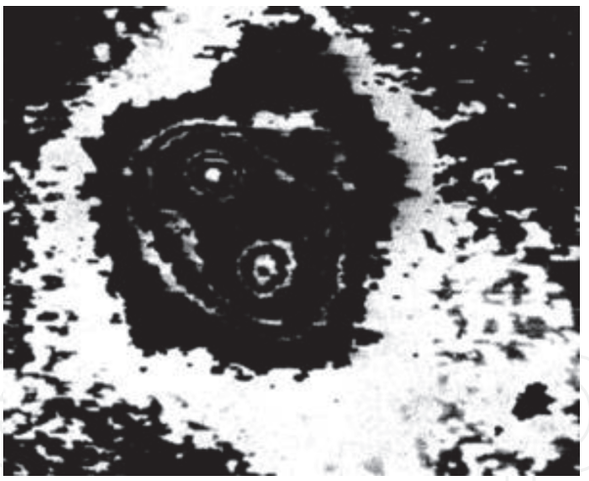

Figure 10.
The isodense picture of the galaxy Markaryan 266 with two nuclei, rotating in the opposite direction [14].

(**Figure 7**). Circulation of substance in different parts of modon occurs in opposite direction (**Figure 4**)!

Now it is difficult to judge about a way of evolution of these structures, for example, whether monopole vortices lead to the formation of planets in circumstellar disks, or the formation of stars or clouds in the galactic gas disk? Or, if it could transformed the dipole vortices to well-known double objects, such as double stars, double nuclei in galaxies (as Mrk 266 [14], **Figure 10**), as well as in giant molecular clouds, or a planet with a companion in circumstellar disk, or not?

As for dusty protoplanetary disks, long-lived anticyclonic vortical structures can capture the ~10 cm to meter-sized particles and grow up them into planetesimals. Let's estimate an order of magnitudes of time (86), and mass (87) for planetesimal formation by Burgers vortex for a model of a disk of radius 30 AU and mass 0.5 $M_\odot$ round a star of solar mass: $M \approx M_\odot$. Taking $R_0 = 20$ AU we will obtain estimations $\Omega_0 \approx 8 \cdot 10^{-9} s^{-1}$ and $\Sigma \sim 1600\, g/cm^2$. For a typical protoplanetary disk at considering distance the vertical scale height is of order $H \approx 10^8$km and sound speed $c_s \approx H\Omega_0 \approx 0.8$ km/s.

Let the maximum rotation speed of a vortex be ~10 m/s at distance $r_0 \approx 10^{10}$m from its center, and converging speed of a stream be $v_r = A \cdot r_0 \approx 5$ m/s. Then we will have

$$\omega \approx 10^{-9} s^{-1}, A \approx 5 \cdot 10^{-10} s^{-1}.$$

The condition (85) is carried out with a large supply for protoplanetary disks. The molecular viscosity of gas, estimated by the formula $\nu \sim \lambda c_s$, in which λ is the mean free path of molecules, c_s is the speed of a sound, does not play an appreciable role in processes of a protoplanetary disk. For this reason, the "α-disk" model [31] is used, in which turbulent viscosity is represented by the expression $\nu \sim \alpha c_s H \approx \alpha H^2 \Omega_0$. The dimensionless parameter α is constant value of an order $\alpha \sim 10^{-2}$. The scale of viscous length thus makes $L_\nu \approx 10^6$km, so Burgers vortex of big sizes cannot be destroyed by viscosity. Keplerian shear length makes $L_{shear} \approx 6 \cdot 10^9$km. Hence, vortices with the sizes $r_{eff} < L_{shear}$ can have circular form.

Taking $\rho * / \rho \approx 10^{10}$ in a midplane of a disk, using in (87) and (86) also the average value for viscosity from stability condition (85), we will receive the estimations:

$$M_p \approx 10^{28} g; \tau \sim 3 \cdot 10^6 (m/D) yrs.$$

Therefore, during an order of $\sim 10^6$ year, for meter-sized rigid particles, in the vortex trunk the mass amount comparable with mass of Venus accumulates.

Finally, note that the disk in the Burgers vortex localization area is thicker.

Author details

Martin G. Abrahamyan[1,2]

1 Yerevan State University, Armenia

2 Yerevan Haybusak University, Armenia

*Address all correspondence to: martin.abrahamyan@ysu.am

References

[1] Hasegawa A, Mima K. Pseudo-three-dimensional turbulence in magnetized non-uniform plasma. Physics of Fluids. 1978;**21**:87

[2] Hasegawa A, Maclennan CG, Kodama Y. Nonlinear behavior and turbulence spectra of drift waves and Rossby waves. Physics of Fluids. 1979; **22**:212

[3] Meiss JD, Horton W. Solitary drift waves in the presence of magnetic shear. Physics of Fluids. 1983;**26**:990

[4] Larichev E, Reznik GM. On the 2D solitary Rossby waves. USSR AS Reports. 1976;**231**:1077

[5] Pavlenko V, Petviashvili V. Solitary waves in a plasma and in atmosphere. Plasma Physics. 1983;**9**:603

[6] Mikhailovskii AB, Aburdzhaniya GD, Onishchenko OG, Churikov AP. Alfven vortex solution in homogeneous magnetized plasma. Journal of Experimental and Theoretical Physics. 1984;**59**:1198

[7] Horton W, Liu J, Meiss JD, Sedlak JE. Physics of Fluids. 1986;**29**:1004

[8] Nycander J, Pavlenko VP, Stenflo I. Physics of Fluids. 1987;**30**:1367

[9] Dolotin V, Fridman AM. Generation of an observable turbulence spectrum and solitary dipole vortices in rotating gravitating systems. Journal of Experimental and Theoretical Physics. 1991;**72**(1):1

[10] Adams FC, Watkins R. Vortices in circumstellar disks. The Astrophysical Journal. 1995;**451**:314

[11] Abrahamyan MG. Vortices in rotating gravitating gas disks. Astrophysics. 2015;**58**:105

[12] Rankine WJM. On the thermal energy of molecular vortices. Philosophical Magazine. 1870;**39**:211

[13] Abrahamyan MG, Matveenko LI. Initial phase of protostar formation. Astrophysics. 2012;**55**:443

[14] Petrosyan AP, Sahakyan KA, Khachikyan EY. Spectroscopic investigation of double nucleus galaxy Markarian 266. Astrophysics. 1980;**16**:621

[15] Heng K, Kenyon SJ. arXiv: 1005.1660v3 [astro-ph. EP]; 2010

[16] Youdin AN. From grains to planetesimals. European Astronomical Society (EAS) Publication Series. 2010; **41**:187

[17] Armitage PJ. Lecture notes on the formation and early evolution of planetary systems. arXiv: astro-ph/ 0701485v2; 2007

[18] Armitage PJ. Astrophysics of Planet Formation. UK: Cambridge University Press; 2010

[19] Blum J, Wurm G. The growth mechanisms of macroscopic bodies in protoplanetary disks. Annual Review of Astronomy and Astrophysics. 2008;**46**:21

[20] Zsom A, Ormel CW, Guttler C, Blum J, Dullemond CP. arXiv: 1001.0488v1; 2010.

[21] Wilner DJ, D'Alessio P, Calvet N, Claussen MJ, Hartmann L. Toward planetesimals in the disk around TW Hydrae: 3.5 centimeter dust emission. The Astrophysical Journal. 2005;**626**: L109

[22] Adachi I, Hayashi C, Nakazawa K. The gas drag effect on the elliptical motion of a solid body in the primordial

solar nebula. Progress in Theoretical Physics. 1976;**56**:1756

[23] Weidenschilling SJ. Formation and evolution of exoplanets. Monthly Notices of the Royal Astronomical Society. 1977;**180**:57

[24] Paterson HL, Feng M, Waite AM, Gomis D, Beckley LE, Holliday D, et al. Physical and chemical signatures of a developing anticyclonic vortexes. Journal of Geophysical Research. 2008; **113**(C7):C07049

[25] Carnevale GF, McWilliams JC, Pomeau Y, Weiss JB. Evolution of vortex statistics in two-dimensional turbulence. Physical Review Letters. 1991;**66**:2735

[26] Weiss JB, McWilliams JC. Temporal scaling behavior of decaying two-dimensional turbulence. Physics of Fluids A. 1993;**5**:3

[27] Tabeling P. Two-dimensional turbulence: A physicist approach. Physics Reports. 2002;**362**:1

[28] Inaba S, Barge P, Daniel E, Guillard H. A two-phase code for protoplanetary disks. Astronomy & Astrophysics. 2005; **431**:365

[29] Inaba S, Barge P. Dusty vortices in protoplanetary disks. The Astrophysical Journal. 2006;**649**:415

[30] Abrahamyan MG. The vortex of Burgers in protoplanetary disk. Astronomical Society of the Pacific. 2017;**511**:254-264

[31] Shakura NI, Sunyaev RA. Black holes in binary systems. Astronomy & Astrophysics. 1973;**24**:337

[32] Pringle JE. Astrophysics of planet formation. Annual Review of Astronomy and Astrophysics. 1981; **19**:137

[33] Chiang EI, Goldreich P. Formation and evolution of exoplanets. The Astrophysical Journal. 1997;**490**:368

[34] Godon P, Livio M. The formation and role of vortices in protoplanetary disks. The Astrophysical Journal. 2000; **537**:396

[35] Abrahamyan MG. Anticyclonic vortex in a protoplanetary disk. Astrophysics. 2016;**59**:309

[36] Chandrasekhar S. Ellipsoidal Figures of Equilibria. New Haven and London: Yale University Press; 1969